Energy Conversion and Management 207 (2020) 112516

Contents lists available at ScienceDirect

Energy Conversion and Management

journal homepage: www.elsevier.com/locate/enconman

Study of thermal insulation materials influence on the performance of thermoelectric generators by creating a significant effective temperature difference

Song Lv[a,b,d,*], Minghou Liu[b], Wei He[c], Xinlong Li[b], Wei Gong[d], Sheng Shen[d]

[a] School of Energy and Power Engineering, Wuhan University of Technology, Wuhan 430063, China
[b] Department of Thermal Science and Energy Engineering, University of Science and Technology of China, Hefei 230026, China
[c] Department of Building Environment and Equipment, Hefei University of Technology, Hefei 230009, China
[d] Department of Mechanical Engineering, Carnegie Mellon University, Pittsburgh, PA 15213, United States

ARTICLE INFO

Keywords:
Thermoelectric generation
Thermoelectric cooling
Material development
Thermal resistance
Thermal management
Efficiency improvement

ABSTRACT

Thermoelectric generator are attractive heat engines because they can convert heat directly into electricity via Seebeck effect. However, the energy conversion efficiency of today's thermoelectric generators is significantly lower than that of conventional mechanical engines. Materials and devices are the main direction of its improvement. Although thermoelectric material has been making some progress, actual thermoelectric devices has remained stagnant with rather poor efficiencies. In this paper, a mathematical model containing heat losses ignored by previous studies are developed and used to discuss how to reduce heat losses to improved thermoelectric performance. In order to reduce and eliminate the impact of heat loss and study the effects of heat loss, the segmented thermoelectric modules filling with different insulation fillers are built to verify the accuracy of the model. Self-made experimental instruments are developed to study of the effect of reducing module heat loss on thermoelectric conversion performance. The results show that the filling of insulation materials makes contribution to the improvement of thermoelectric performance, the efficiency of aerogel filled module is 8.225% higher than that of unfilled module, and the efficiency of thermoelectric module can be improved up to 9.12% by adding ideal thermal insulation materials. The results also showed that the performance of TE module depends on the thermal conductivity of filling materials and its' filling rate. Those results provided some practical guidelines for the design and improvement of practical thermoelectric modules.

1. Introduction

With the rapid development of the economy and industry, the problems related to environment and energy gradually drew worldwide attentions. How to meet future energy demand in a renewable and sustainable manner is a major global challenge of the world. Thermoelectric (TE) technology is seen as an alternative and environmentally friendly technology for directly converting heat into electric power, based on the Seebeck effect. Thermoelectric generators (TEGs) have no moving parts, no chemical reaction, no noise, no pollution, maintenance free, long-term reliability and easy adjustment of device or equipment size [1]. So they have been attracting more and more attention from both the academic and industrial communities [2]. The earliest range of stove applications was extended to aerospace applications, transportation vehicles, medical instruments, industrial facilities, electronic equipment, sensing instruments, power plants, factories, automobiles, computers, renewable energy and even the human body [3,4]. Although TE technology has been around for more than a century and has been used in specialized fields, low efficiency and high cost have hindered the widespread application and commercialization of thermoelectric technology [5]. The efficiency of ideal TEG η is determined by their operating temperature and the TE materials' dimensionless figure of merit (ZT). It could be written as [6],

$$\eta = \frac{T_h - T_c}{T_h} \cdot \frac{\sqrt{1 + ZT} - 1}{\sqrt{1 + ZT} + T_c/T_h} \quad (1)$$

where T_h is the hot-side temperature, T_c is the cold-side temperature, and ZT is the effective ZT of the thermoelectric material between T_h and T_c.

Over the past two decades, although the improvement of thermoelectric materials has made significant progress and extensive research efforts have been made to improve the performance of TE materials,

* Corresponding author at: School of Energy and Power Engineering, Wuhan University of Technology, Wuhan 430063, China.
E-mail address: lvsong@mail.ustc.edu.cn (S. Lv).

https://doi.org/10.1016/j.enconman.2020.112516
Received 14 August 2019; Received in revised form 15 January 2020; Accepted 17 January 2020
Available online 09 February 2020
0196-8904/

Nomenclature

A_i	area, m^2
A_{teg}	area of TE module, m^2
E_e	heat convert into electricity, J
E_{b1}	heat loss from edges, J
E_{b2}	heat loss from back side, J
E_{b3}	heat loss from ceramic substrate, J
E_{bi}	radiant heat from each part of TEG, J
F_i	fill factor
I	current, A
k_f	thermal conductivity of fillers, W/(m·K)
L_{fi}	length of fillers, m
M_i	quality of materials, g
P	electric power, W
Q_{teg}	heat conducted into the top of the TEG, J
Q_{in}	heat absorbed by the hot side surface of TEG, J
$Q_{teg,c}$	heat rejected by the cold side surface of TEG, J
Q_{h1}	convective loss from thermoelectric elements, J
$Q_{\eta 1}$	heat conducted through filler material, J
q	heat flux density, J/(㎡·s)
S	Seebeck coefficient
T_h	hot-side temperature, K
T_c	cold-side temperature, K
V	open circuit voltage, V
x	length in calculation field, m
ZT	dimensionless figure of merit of TE materials

Greek symbols

β	heat conduction of air, W/(m·K)
δ	Stefan-Boltzmann constant
ε_c	emissivity values of cold side surface
ε_h	emissivity values of hot side surface
ρ	density of filler material, kg/m3
η	energy efficiency of ideal TEG

pushing ZT values over 2–3 with the help of nanotechnology, the actual TE module has progressed less rapidly and remained stagnant with rather poor efficiencies which far behind inherent efficiency of TE materials (as shown in Eq. (1)) when it comes to real-word application of thermoelectric technology for direct thermal to electricity conversion. The reason is that thermoelectric materials used for heat engines or heat pumps in practice need to be fabricated and integrated to module based on the requirements. Due to the less than optimal device structure and the existence of various electrical losses and heat losses, the conversion efficiency of fabricated TE modules is much lower than the theoretical efficiency based on the performance of TE materials themselves [7–9]. Thus, in addition to the interest in enhancing the thermoelectric properties by improving the competitiveness of thermoelectric materials, another direction is by improving the actual thermoelectric module [10–12]. In order to improving TE module efficiency, strenuous efforts have focused on the optimization of both the element, geometric and component issues such as metallization layers, thermoelectric legs and insulating plates to minimize energy losses in recent years by simulations and experiments [13–19]. These improvements doesn't involve the figure of merit (ZT) of thermoelectric material improvements at all, which actually improve thermoelectric performance by reducing energy loss and increasing the effective temperature difference across the thermoelectric elements ΔT according to Eq. (1). It is generally believed that as less heat is lost and more heat is forced through the thermoelectric legs, their performance increases [20–24]. Thus, the heat loss between the thermoelectric legs, substrates and some other components must be carefully considered and analyzed in the design of thermoelectric modules and devices. But the previous studies always ignore the heat leakage through the thermoelectric elements by assuming that the TEG is thermally isolated from the surroundings except for the heat flows at the thermoelectric elements. And various heat losses are ignored in simplifying structural or calculation process which leads to very different results [25]. There are only a few studies have paid special attention to this issue. Through simulation calculation, Zebarjadi [26] proved that insulations are used to minimize the heat losses and therefore to increase the overall efficiency and achieve larger electric power output. Zhang et al. [27] demonstrated a three-dimensional numerical analysis model of a segmented TE device, which takes into account various parasitic losses. Based on the numerical analysis model and the extremely low heat losses, they realized a thermoelectric conversion efficiency of 12% TE modules. Lee et al. [28] developed a mathematical model considering temperature dependent material properties and thermal losses and interfacial resistance inside the device, for a thermoelectric generator (TEG) to analyze temperature dependent performance in terms of output power and efficiency. The results shown that analytical equations with effective properties can provide excellent estimation of the performance of a TEG over a certain operating range, and the results have not been verified by experiments. Li et al. [29] simulated thermoelectric performance of SiGe unicouple filled with four kinds of thermal insulation materials to eliminate the heat loss. The results showed that the conversion efficiency η of SiGe thermoelectric legs is ~7.5% at T_h = 1223 K (1173 K) and Tc = 573 K. Thus, those studies based on numerical simulation has its own limitations in terms of its application in a different temperature environment and structure parameters.

Here, on the above analysis, this work studied the heat loss between

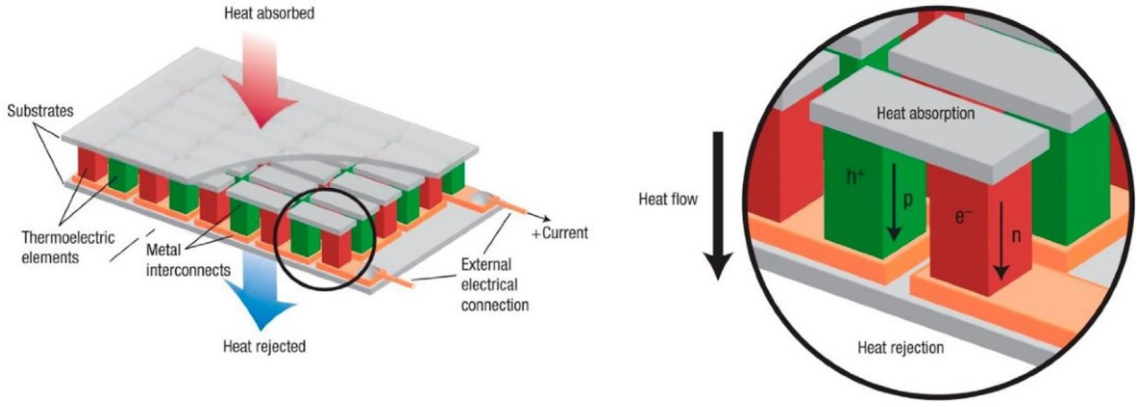

Fig. 1. Schematic drawing of a thermoelectric generator; according to [30].

the thermoelectric legs and substrates in the actual TE modules influence on the performance of it by theoretical analysis and experiments. First of all, an analytic model considered various thermal losses of an actual TE module has been carried out. Apart from considering heat losses by conduction, radiation and convection within the real TE module, thermal radiation from hot to cold plate and leg are all considered. Thermal insulating materials are used to fill the gaps between the TE legs to isolated reduce heat leaks at the legs. Based on the multi-parameter optimization process, a mathematical model with the filling rate (the ratio of the thermoelectric legs and the filling material) and the thermal conductivity of the filling material and the thermal conductivity of the ceramic insulator are established. Combined with the filling rate and module assembly method, a full-parameter computer simulation based on MATLAB was performed. Secondly, four typical types of thermal insulation materials including aerogel, glass fibers, Min-K and air are used as fillers in actual TE module manufacturing, and their effect on thermoelectric performance were investigated by experiment. In addition, the filling rate of the thermal insulating materials, F, is introduced and measured. The accuracy of the model is verified via a simple numerical simulation and an experiment. Experimental measurements show good agreement with simulation results. Furthermore, the performance of TE modules affected by the insulating materials, the filler's thermal conduction and filling ratio were evaluated and predicted. Finally, based on the results of overall emulation to experiment, this work proposes a design basis and guidance for improving the practical of a real TE module.

2. Models

The most common design of a TE module is shown in Fig. 1. The metal interconnect is printed on an alumina oxide substrate. Most importantly, on top of every one of these (copper) interconnections are: a p- and an n-type thermoelectric leg, which the combination of a p- and an n-type leg is called a thermocouple. Inside the thermoelectric generator, many thermocouples are connected in series and thermally connected in parallel. At the top of the generator connected a further substrate. The two substrates must be parallel because they establish the thermal interface of the generator. The heat flows through the substrate, so this design is called a cross section. Most of the generators currently available on the market fall into this category. A typical real thermoelectric module is shown in Fig. 2.

Ideally, the heat flux from heat resource crosses the substrate and metal interconnections to the thermoelectric elements. The energy balance for the hot side is shown in Fig. 3.

The steady-state energy balance on the hot side of the TE module details the loss of thermal efficiency,

$$Q_{teg} = Q_{in} - E_e - Q_{teg,c} - E_{b1} - E_{b2} - E_{b3} - Q_{h1} \tag{2}$$

Here, Q_{teg} is the heat conducted into the top of the TEG; Q_{in} is the heat absorbed by the hot side surface of TE module; E_e is the heat convert into electricity. The last four terms on the right hand side of Eq. (3) is the convective loss and radiation loss from the heat resources, edges, back side, ceramic substrate and thermoelectric elements, which leads to smaller temperature difference across the thermoelectric element and was neglected of most models in the simulation. In previous studies, in order to minimize losses, the system were placed in a vacuum enclosure to eliminate the last three items, air conduction/convection losses. But the radiation loss can't be eliminated. In order to get a high efficiency, a high temperature difference is needed, which lead to a large radiation heat loss.

In the absence of insulating filler, there will be thermal radiation between the cold and hot ends in the unicouple. According to Stefan Boltzmann's law, radiant heat can be estimated by the following formula [31]:

$$E_{bi} = \frac{A_i \times 10^{-4}\delta(T_h^4 - T_c^4)}{1/\varepsilon_h + 1/\varepsilon_c - 1} \tag{3}$$

where δ is Stefan-Boltzmann constant, $\delta = 5.67 \times 10^{-8}$ W m^{-2} K^{-4}; A_i is space area between legs, which could be calculated by subtracting TE legs cross sectional area from total cross sectional area. ε_h and ε_c are emissivity values of hot and cold side surfaces, respectively.

The gap between the legs of the thermoelectric module could be filled with some filler to avoid packing, mechanical support or radiation shielding. The filler generates thermal bypass,

$$Q_{\eta 1} = k_f A_{fi} \frac{T_h - T_c}{L_{fi}} \tag{4}$$

Here, in order to reduce the radiation and convective heat losses in the actual TE module, the gap between the TE legs is filled with an insulating material (as is shown in Fig. 4).

First, the performance characteristics (efficiency, hot junction heat input, electrical power output, etc.) of the individual thermoelectric legs are calculated using the temperature-dependent properties of the thermoelectric materials and Domenicali's coupled 1st order equations which are modified to include the effect of leg radiation heat loss, conduction through the gaps (convection of the gaps is neglected due to narrow space) and the thermal cross talk between the two interim surfaces of the substrates by radiative heat transport [32].

$$\frac{dT}{dx} = \frac{i(ST)_x - q_{leg}(x)}{k(x)} \tag{5}$$

$$\frac{dq_{leg}}{dx} = \left[i\rho(x) + S(x)\frac{i(ST)_x - q_{leg}(x)}{k(x)} \right] i - \frac{Pq_{rad}(x)}{A_{leg}} - \frac{\beta_{air} T_x}{A_{te} - A_{leg}} \tag{6}$$

The first-order equations for these couplings are the optimal thermoelectric heat flow and temperature distribution for the N-type and P-type components that are iteratively solved for the optimum current density for a particular TEG geometry.

The differentiating energy balance equation for the thermoelectric elements is:

$$\frac{\partial}{\partial x}\left(\kappa(x)\frac{\partial T(x)}{\partial(x)} + \kappa_F(x)\frac{\partial T_F(x)}{\partial(x)} \right) = -\rho J^2 + JT(x)\frac{\partial S(x)}{\partial x} \tag{7}$$

It can be solved by iterative techniques to decompose the equation into a set of coupled differential equations (Eq. (7)) [33].

$$\frac{dT}{dx} = \frac{TSJ - q}{\kappa} \tag{8}$$

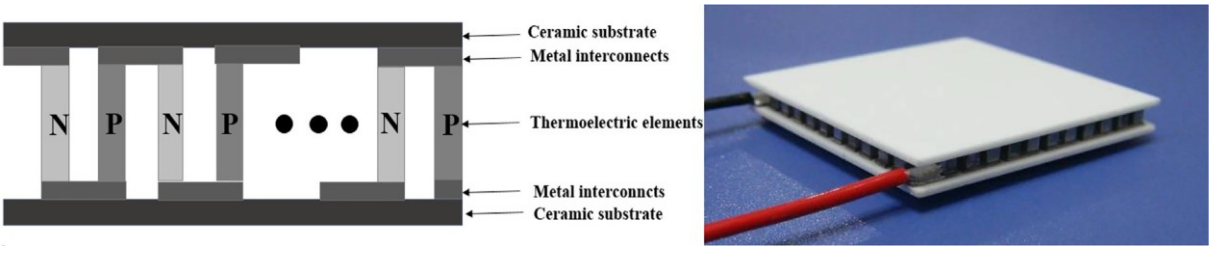

Fig. 2. (a) Schematic diagram of thermoelectric module, (b) Picture of a real thermoelectric module.

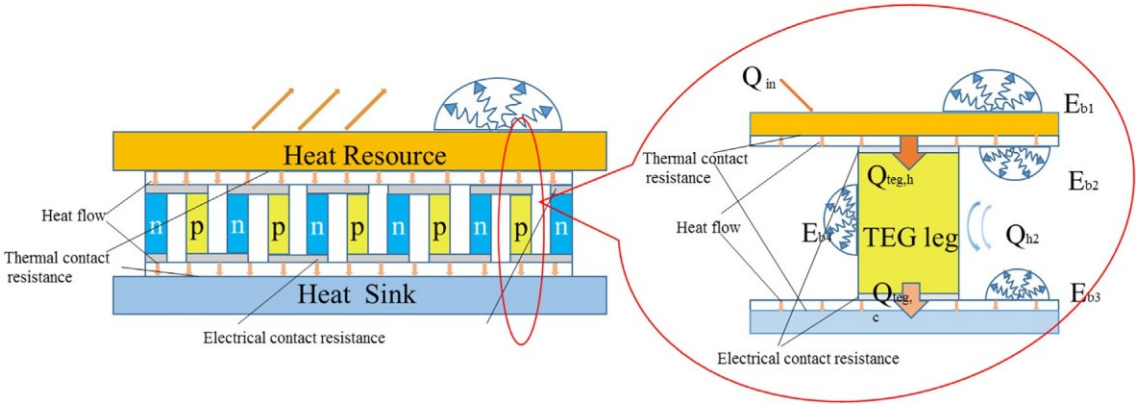

Fig. 3. TEG schematic illustrating heat flows.

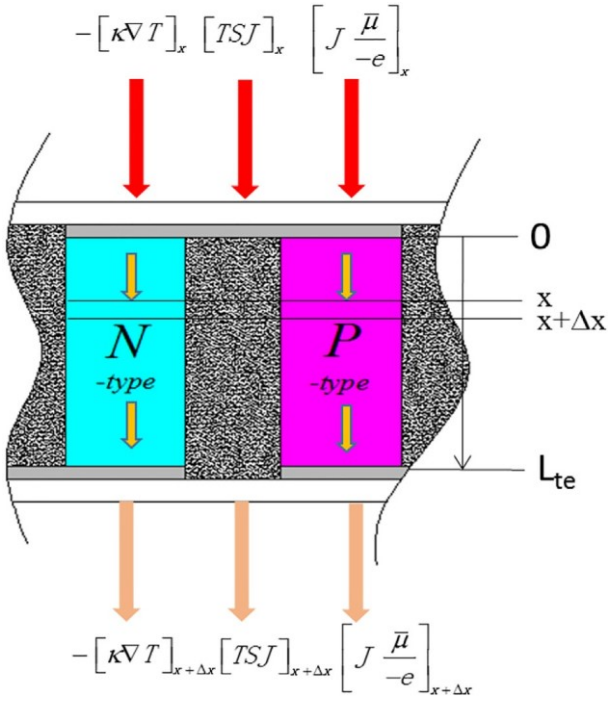

Fig. 4. Discretization of thermoelectric elements for numerical simulation of filled TE module.

$$\frac{dq}{dx} = \rho J^2 + SJ\frac{TSJ - q}{\kappa} \tag{9}$$

These equations can be numerically solved to obtain the temperature distribution and heat flux distribution inside the thermoelectric element, as well as the power output and efficiency of the component. This basic framework for determining the performance of a thermoelectric element can be used to determine the efficiency of a TEG filled with a thermoelectric element.

The entire model also considers the thermal contact resistance and electrical contact resistance at the interface. To predict the upper limit of efficiency, the solder is ignored and all contact resistances are set to zero.

$$k_{te}\frac{d^2T_e}{dx^2} + j_e^2\rho_e - \frac{Pq_{rad}(x)}{A_{leg}} - \frac{\beta_{air}T_x}{A_{te} - A_{leg}} = 0 \tag{10}$$

The boundary conditions for the differential equations of the two thermoelectric elements are the same fixed cold and hot end temperatures that uniquely determine the optimum current, temperature, and heat flux distribution for a particular single even TEG geometry.

$$T|_{x=L_{te}} = T_c \tag{11}$$

$$T|_{x=0} = T_h \tag{12}$$

$$T(x) = T_h - \frac{x}{L_{te}}(T_h - T_c) - \frac{\rho_{te}j_{te}^2}{2k_{te}}x(x - L_{te}) \tag{13}$$

The temperature gradients at the junction are obtained by solving the differential equations governing thermoelectric transport inside each of the thermoelectric elements

$$-k_{te}\frac{dT(x)}{dx}|_{x=0} = \frac{k_{te}}{L_{te}}(T_h - T_c) - \frac{\rho_{te}j_{te}^2}{2k_{te}}L_{te} \tag{14}$$

$$-k_{te}\frac{dT(x)}{dx}|_{x=L_{te}} = \frac{k_{te}}{L_{te}}(T_h - T_c) + \frac{\rho_{te}j_{te}^2}{2k_{te}}L_{te} \tag{15}$$

These equations include temperature dependent thermoelectric properties.

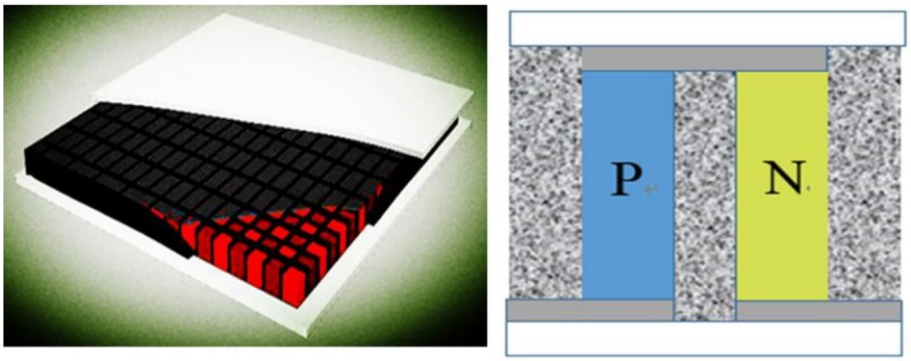

Fig. 5. The schematic diagram of the filled thermoelectric module.

Thermoelectric conversion efficiency is obtained by:

$$\eta = \frac{P}{Q_h} = \frac{P}{P + Q_c} = \frac{IV}{IV + Q_c} \times 100\% \quad (16)$$

The equations are solved numerically and presented in Fig. 5 to compare with experimental data.

3. Experimental verification

A novel experimental setup was developed to characterize the thermal properties of the filling thermoelectric modules and verify the accuracy of the mathematical models. Significant effort went into creating a repeatable setup that would accurately validate the assumptions made in the theoretical model so as to reliably compare the measured results with the manufacturer's given performance specifications.

3.1. Fabrication of the filling thermoelectric modules and the filling factor

To explore how filling materials affect thermoelectric performance of TE modules, we fabricated three prototype TE modules with a total of 71 pairs of n–p Bi_2Te_3-based materials (see Fig. 6). The three TE modules filled with different kinds of thermal insulation materials are achieved by using TEGs based on commercially available thermoelectric legs consisting of bismuth telluride thermoelectric materials, which was provided by Ferrotec Holdings Corporation. First, the Bi_2Te_3 material is diced into the desired size and connected with the metal connections by soldering, and brazing to a Cu electrode. Second, in order to reduce the radiation and convection heat losses in the module, the gap between the legs is filled with a heat insulating material having a low thermal conductivity. For our research, the most suitable thermal insulation materials available on the market, considering maneuverability, meshed with solid thermoelectric element, three kinds of thermal insulation materials including Min-K [17], aerogel [18], and ceramic fiber [19] were chosen. Temperature-dependent thermal properties are shown in Fig. 7. The overall fabrication process of a filling TE module in the current study is shown in Fig. 8. A prototype TE module which was unfilled with thermal insulation materials (It can also be thought to be filled with air) are fabricated for comparison. The four TE modules with dimensions of 40 × 40 × 3.5 mm^3 were marked as module I, module II, module III, and module IV were fabricated. The typical parameters used for the models are summarized in the following Table 1 and Table 2.

Here, we define the fill factor F_i as the ratio of actual fractional area coverage of the thermal insulation materials to the corresponding the gaps area between the thermoelectric legs (thermoelement) $F_i = A_{teg}/(A_i + A_{teg})$. In experiments, we get it like this. First, we calculate the theoretical filling amount (M_t) by geometric parameters and filling materials density. Then, filling material quality filled into the gap (M_m) are accurate measured, and we get the fill factor $F_i' = M_m/M_t$. Finally, we compare F_i and F_i', and get corrections to get F_i.

3.2. The experimental setup

An experimental setup was designed and utilized to measure the thermoelectric properties and output power of TE modules, which is seen in Fig. 9. The setup consists of a thermoelectric module sandwiched between two copper plates. The sample (4 cm by 4 cm in area) is placed between the two blocks. Four type K thermocouples are embedded into the top copper block with 1 cm separation between thermocouples. The other 4 thermocouple in the bottom copper block to measure the temperature difference across the face of module. This is used to validate the assumption of a constant temperature across the face of the device. Subtracting the difference. Both sides of the two copper blocks are covered with a heat insulating material, and both surfaces in contact with the sample are polished to reduce the contact resistance. Thermal energy is provided by five cartridge heaters capable of producing 2000 W maximum. The cartridge heater, essentially a precision, temperature-constant resistive element, is installed inside a mild steel sheath to allow for more even temperature distribution and is powered by an external transistor hooked up to a standard 120 V wall outlet.

A cold water heat exchanger was used the cold side of the module. A thermoelectric cooler was used as the heat sink to control the cold side temperature and heat flux of TE module. Surrounding the rest of the setup was an insulating Plexiglas box that not only used to minimize heat loss also helped to create a repeatable environment for the measurements. Use voltage sensors, current sensors, and data loggers to measure and record relevant data. DC power supply and control circuit were set to run the entire experimental device. The experimental group and the control group of TE modules were tested in steady state and dynamic conditions with the electric heating power and a rheostat as the load of the TE modules.

3.3. Experimental verification

The prototype TE modules were tested using a home-built testing system described above. The test samples (module I, II, III, and IV) were placed between two copper blocks in sequence and fixed by the weight of the top copper block. Four thermocouples are inserted into each of the copper blocks with a fixed spacing between the thermocouples. Five cartridge heaters are inserted into the top copper block. A thermoelectric cooler was placed under the copper block at the bottom and was run continuously throughout the experiment. Due to imperfect contacts, the thermal resistance between the TE module and the external heat source/cold source inevitably exists and causes an additional temperature drop, thereby reducing the effective temperature difference across the TE element. Through the calibration experiment, the true temperature of the cold and hot ends of the module at different heat source temperatures is obtained. The current, terminal voltage, and output power were measured at different temperature differences (ΔT) with a heater temperature (Theater) of up to 400 °C. The cold side was cooled using circulating water at a fixed temperature of 5 °C. In order to obtain maximum thermoelectric output, a rheostat was used as the load of each TE module in the experiment with the same temperature difference. We get the electrical characteristics of each TE modules by change the resistance at different values in the range 0–15 Ω. The uncertainty of the thermocouples, and other measuring equipments are listed in Table 3.

A MATLAB code provided the same properties of materials, heat fluxes with the experiment has been written to simulate the thermoelectric performance. The comparison between the experimental results and that of the model permit to validate the accuracy of model. The variation of the output as a function of external electric load are presented in Fig. 10. The results showed that the model agrees well with

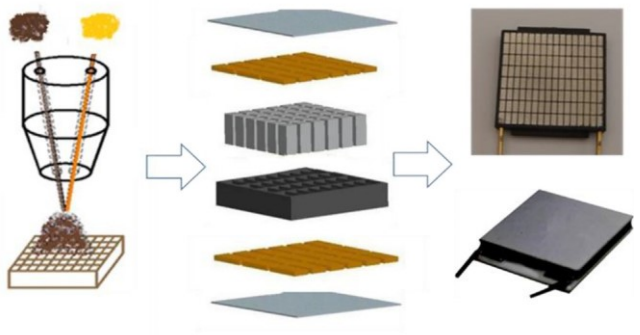

Fig. 6. The overall fabrication process of a filling TE module.

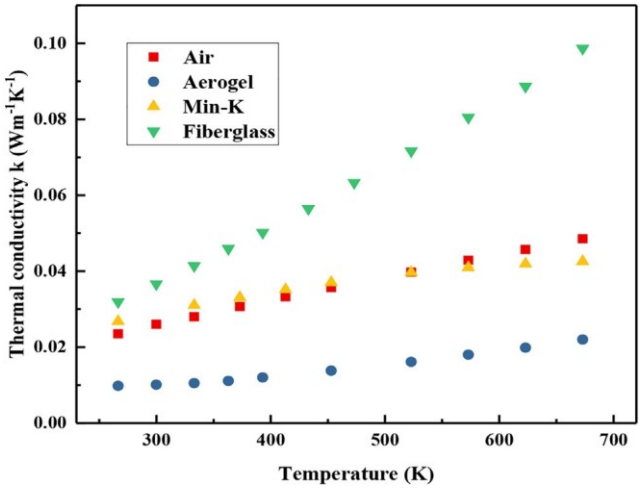

Fig. 7. Temperature-dependent thermal properties of the filling materials.

the experiment results. And it also indicate that the internal resistance of the integrated TE modules is approximately 6.15 Ω. In addition, other filled TE modules are tested the same way. The variation of the thermoelectric characteristics for an electric load of 6.15 Ω of the TE modules as a function of the temperature difference is shown in Fig. 11. As shown in Fig. 11a and Fig. 11b, the experimental data for output power agrees well with the simulated results, while fully accounting for the heat loss, interfacial heat transfer coefficients and fillers. As is shown in Fig. 11b, test results are consistent with simulations, and the maximum error between experiment and simulation is 5.187%, fully demonstrating the reliability of the model. The comparison between the experimental results and that of the model permit to validate the accuracy of model.

4. Discussion and perspectives

In order to study the effect of filling materials on the performance of the integrated TE module, and to improve the efficiency of the TE module by reducing heat loss, we also experimentally studied the effect of the insulating filler filled in the integrated module. The module is tested under the same experimental steps as the verification process. The results are shown in Fig. 12.

And it is obvious that the filled modules have higher output power and efficiency compared to unfilled modules. The maximum output power is 8.225% higher than there is no fillers in the space between legs. This is especially evident at high temperatures, which confirms the effectiveness of the filler in reducing radiation and convective heat losses. The output efficiency of TE module increases with the decrease of the thermal conductivity of fillers (k_F). This could be caused by the reduction or elimination of thermal radiation/convection through the element gaps so that all heat goes through the thermoelectric legs. Furthermore, with the increase of temperature difference, the increase of output performance of different modules is also increasing. In the previous studies, many of them explained the increasing disparities as increased radiation heat loss due to temperature rise. But in our experiments we can find that radiation heat loss between thermoelectric legs and substrates accounts for only a small part of it and almost negligible. Because the performance of Min-K filled module is similar to the unfilled module in the experimental range. The thermal conductivity of fillers (k_F) of Min-K is approximately equal to that of air which is the fillers in the unfilled module (as is shown in Fig. 7.). The influence of radiation heat loss on performance is not more than 1%, which can be neglected.

When the thermal conductivity of fillers is lower than that of air. The filling materials filled the gaps between the TE legs to diminish heat losses will generate other thermal bypasses. The thermal bypasses will consume part of the input heat flow, degrade the thermoelectric performance.

As is shown in Fig. 13, the effect of the thermal conductivity of the fillers (κ_F) on the performance of TE modules were given by the mathematical model verified by experiments. Under the same filling rate and filling conditions, with the increase of the thermal conductivity of fillers, the open circuit voltage V_{oc} gradually decrease due to the increased of thermal bypasses. The maximum output power P_{max} decrease slowly due to the heat leakage from bypass. When the thermal conductivity of filler exceeds that of thermoelectric material, the efficiency decreases sharply with the increasing thermal conductivity filling materials because most of the heat will come from the filling material path.

Fig. 14 showed when an ideal thermal insulation material (the thermal conductivity of material is less than 0.01 W/m K) has been filled into the TE module, the effect of the filling rate on the performance of the integrated TE modules. With the increase of the filling rate, the temperature of the hot side increase while the temperature of the cold side decrease. That is because the absorbed heat (Q_h) and rejected heat (Q_c) both reduced with the addition of thermal insulation material. $F_i = 1$ means the fractional area coverage of a thermoelement is large less than substrate area filled by insulation material. The efficiency increases rapidly with increasing of filling rate at low fill factors because the effect thermal flux through the thermoelectric legs is increase which is mainly because that the κ of thermoelectric materials is larger than that of the thermal insulation filler. At large than 0.3 of filling rate, the heat transport is significantly limited by the heat flow through thermoelectric legs. For fill factors as large as 0.35, there is an optimal filling rate corresponding to the maximum efficiency.

For fill factors as large as 0.7–1.0, the heat transport is significantly limited by the spreading resistances so that the efficiency tends the reduction. And the closer the fill rate is to 1.0, the faster the efficiency decreases. Due to Joule heat and Thomson effect increases inside the TE elements. This result indicates the advantage of using an optimal fill factor (0.1–0.35, and that one can essentially reduce the leg material and effectively improves performance.

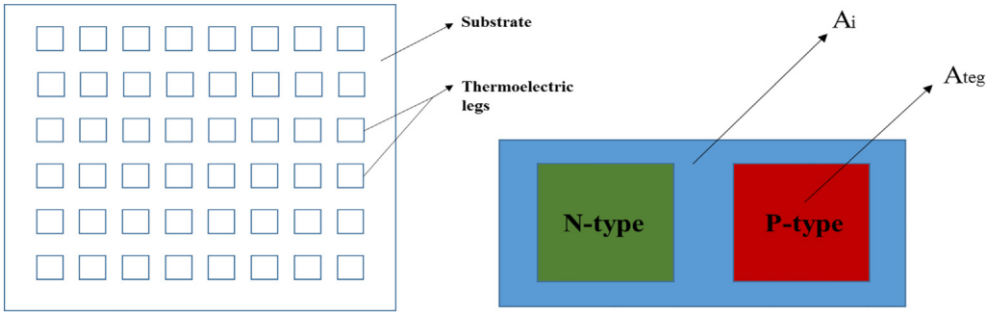

Fig. 8. Geometrical configuration showing n- and p-legs on the TE modules.

Table 1
Details regarding material's parameters used in the manufacturing and analysis.

Items	Materials	Thermal conductivity (W m^{-1} K^{-1})	Electrical resistivity (Ohmm m^{-1})
Insulating ceramic plate	AlN	200	–
Contact layer	Ni	90	6.25×10^{-8}
Thermoelectric legs	Bi_2Te_3	~0.1–1.5 (15–300 °C)	$\sim 3.35 \times 10^{-8}$
Electrode	Cu	380–260 (3–150 °C)	1.68×10^{-8}
Heat conduction	Thermal glue	1.7	–
Without fillers	Air	0.026	–
Filler 1	Glass fibers	~0.08	–
Filler 2	Aerogel	~0.01	–

Table 2
Details regarding the dimension of the filling TE module.

Items	Parameter	Numerical
TE module	Length × width × height	40 mm × 40 mm × 3.9 mm
	Numbers of P or N junction n	142
n-type leg	Cross-section area	1.6×10^{-5} m^2
	Height	3.4×10^{-3}
p-type leg	Cross-section area	1.6×10^{-5} m^2
	Height	3.4×10^{-3}
gap	Width	3×10^{-3}

Table 3
The uncertainty of the equipment.

Test equipment	Uncertainly
Voltmeter	±0.3%
Ammeter	±0.1%
Thermocouple	0.1–0.2 K

5. Conclusion

In this work, the effect of heat loss through the thermoelectric elements on thermoelectric modules has been studied both numerically and experimental. By filling four typical types of thermal insulation materials in actual TE module, we studied optimizing the integration module and reducing the heat loss of devices to improve device efficiency under different conditions. Both experiment and simulation calculation were provided an objective design choice for a real more efficient TE module.

The results show that, (1) in a real TE module, there are indeed problems of decreasing effective temperature difference and inefficiency due to internal heat loss.

(2) Filling thermal insulation material is a very effective way to reduce heat loss and improve module efficiency in the manufacture of practical TE modules. In our experiment, the efficiency of aerogel filled module is 8.225% higher than that of un filled module. And ideal thermal insulation material can increase the efficiency of modules by up to 9.12% according to the simulation.

(3) Furthermore, through the contrast experiment of specific filling

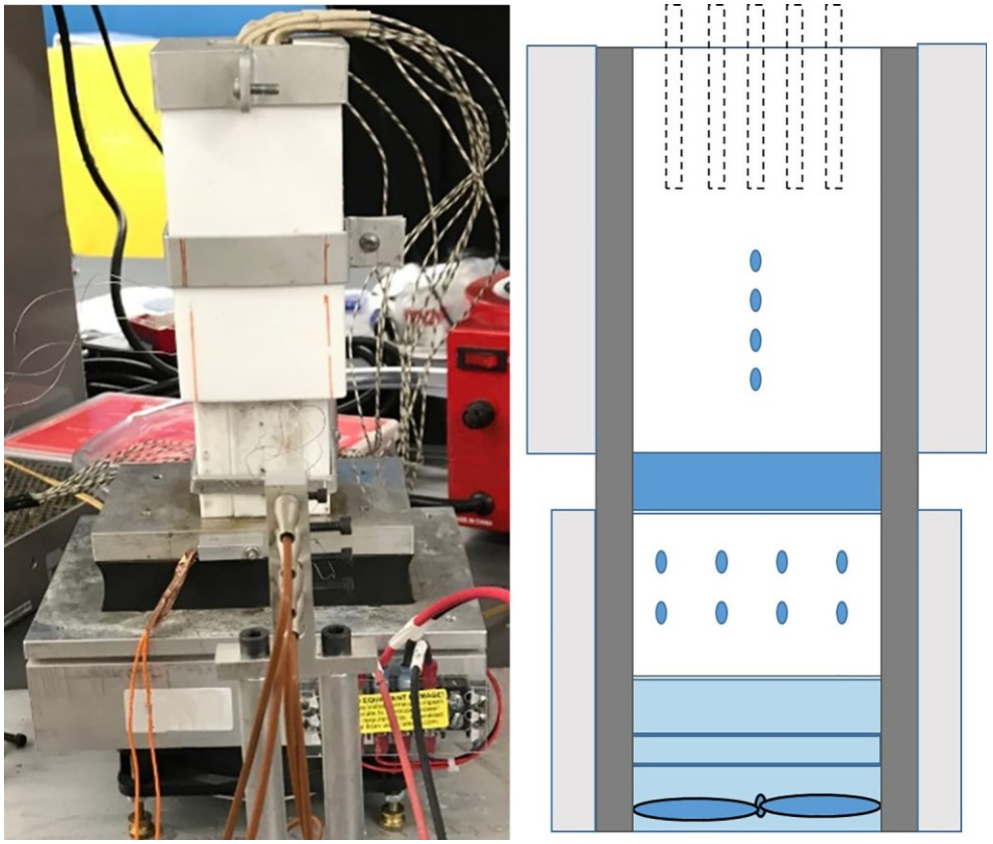

Fig. 9. (a) Schematic of the main testing device, (b) Picture of the main testing device.

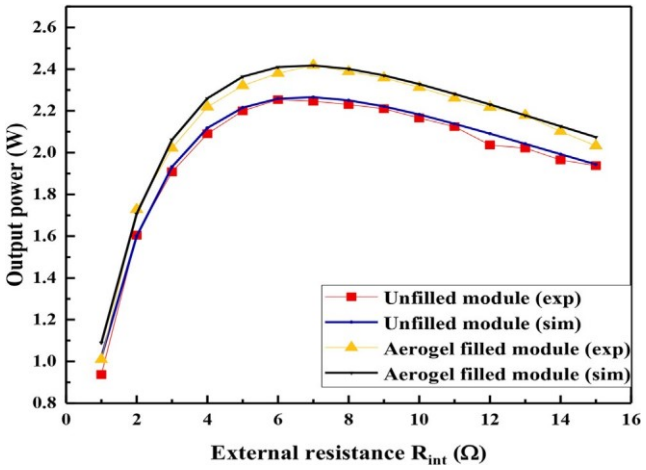

Fig. 10. Change in output power with an external load.

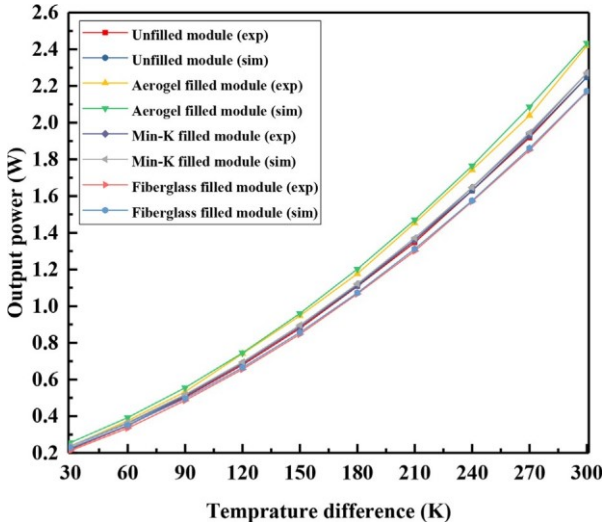

Fig. 11a. The output power of experiment and simulation varies with the temperature difference.

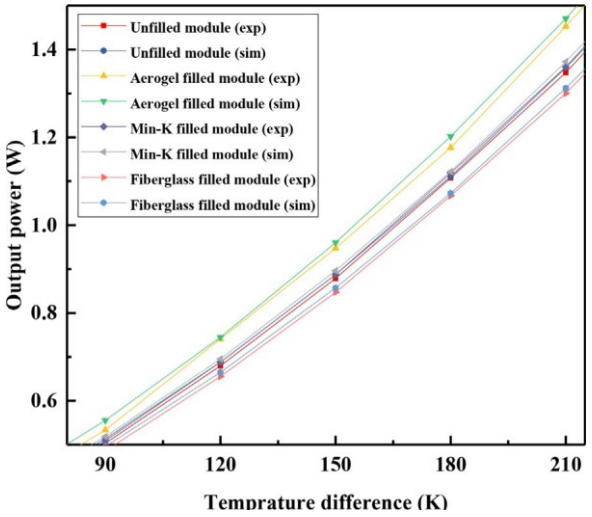

Fig. 11b. Local amplification of change in output power with the temperature difference.

material and no filling material, we found radiation heat accounts for only 1.2–9.6% of heat loss, and heat flow from gap between

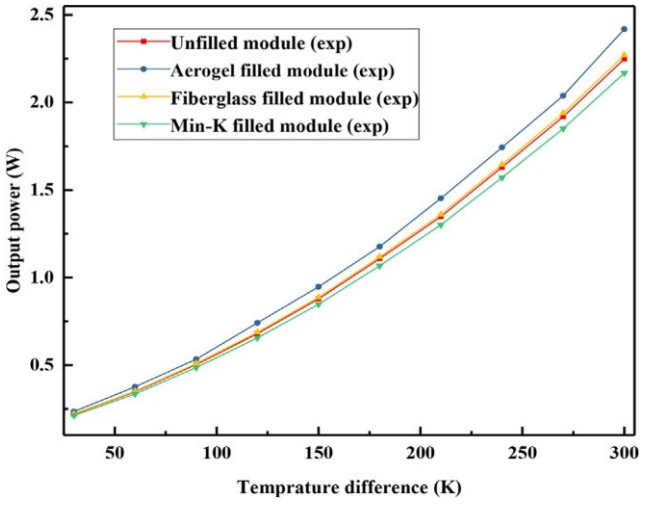

Fig. 12. Change in output power with the temperature difference.

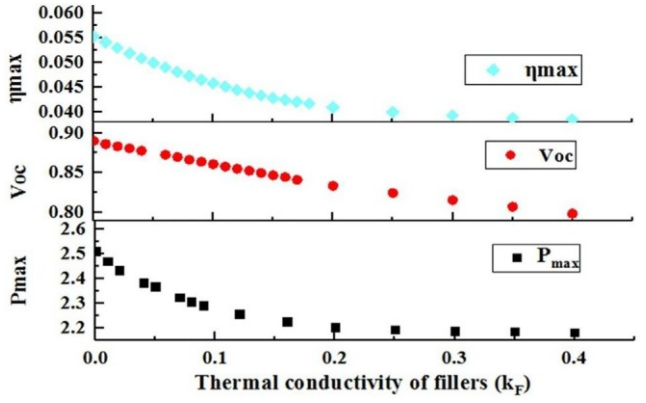

Fig. 13. The effect of the thermal conductivity of fillers on the performance of the integrated TE modules.

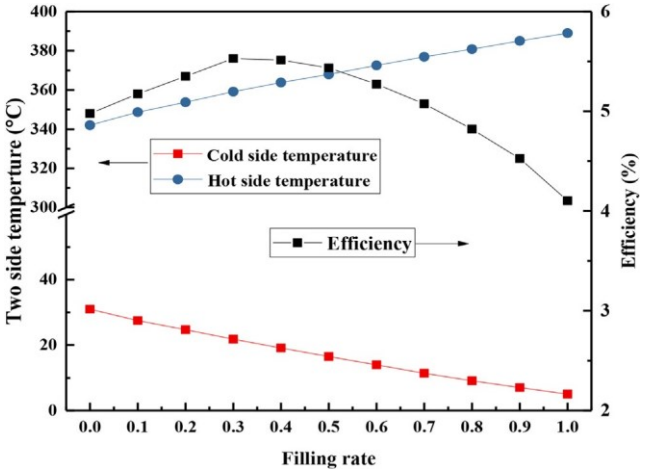

Fig. 14. The effect of the filling rate on the performance of the integrated TE modules.

thermoelectric legs will lead to a η decrease of 0.1–1.32%, where the effective temperature will decrease of 1–2.24%.

(4) Considering the fractional area coverage of the filling materials, ie, fill factor, in a integrated module, the fill factor as large as 0.1–0.35 provides an even more dramatic improvement to performance of the TE module. That is, relatively small and wide thermoelectric legs and relatively compact space make contribution to the TE modules' output

efficiency.

(5) This benefit suggests the technological challenges for the next development steps in construct a high performance TE modules with a good insulating material between the thermoelectric elements and a significant reduction in thermoelectric material with an optimal filling rate.

CRediT authorship contribution statement

Song Lv: Conceptualization, Methodology, Validation, Investigation, Writing - original draft, Writing - review & editing, Supervision. Minghou Liu: Methodology, Project administration, Writing - review & editing, Funding acquisition. Wei He: Formal analysis, Funding acquisition, Writing - review & editing. Xinlong Li: Software, Validation, Data curation. Wei Gong: Methodology, Investigation, Visualization. Sheng Shen: Conceptualization, Methodology, Resources.

Declaration of Competing Interest

The authors declare that they have no known competing financial interests or personal relationships that could have appeared to influence the work reported in this paper.

Acknowledgment

The study was sponsored by the Fundamental Research Funds for the Central Universities (WK6030000071), the grants from Science and technology cooperation project of Qinghai Province (No. 2017-HZ-807), Beijing advanced innovation center for future urban design (No. UDC2016040200), and also Independent innovation fund project of Wuhan University of Technology (No. 203105003).

References

[1] Champier D. Thermoelectric generators: a review of applications. Energy Convers Manage 2017;140:167–81.
[2] Lv S, He W, Hu D, Zhu J, Li G, Chen H, et al. Study on a high-performance solar thermoelectric system for combined heat and power. Energy Convers Manage 2017;143:459–69.
[3] Yang L, Chen ZG, Dargusch MS, Zou J. High performance thermoelectric materials: progress and their applications. Adv Energy Mater 2018;8(6):1701797.
[4] Bell LE. Cooling, heating, generating power, and recovering waste heat with thermoelectric systems. Science 2008;321(5895):1457–61.
[5] Vining CB. An inconvenient truth about thermoelectrics. Nat Mater 2009;8(2):83–5.
[6] Rowe DM. Thermoelectrics handbook: macro to nano: CRC press, 2005.
[7] Kim SI, Lee KH, Mun HA, Kim HS, Hwang SW, Roh JW, et al. Dense dislocation arrays embedded in grain boundaries for high-performance bulk thermoelectrics. Science 2015;348(6230):109–14.
[8] Hu X, Jood P, Ohta M, Kunii M, Nagase K, Nishiate H, et al. Power generation from nanostructured PbTe-based thermoelectrics: comprehensive development from materials to modules. Energy Environ Sci 2016;9(2):517–29.
[9] Ferrario A, Boldrini S, Miozzo A, Fabrizio M. Temperature dependent iterative model of thermoelectric generator including thermal losses in passive elements. Appl Therm Eng 2019;150:620–7.
[10] Ferreira-Teixeira S, Pereira A. Geometrical optimization of a thermoelectric device: numerical simulations. Energy Convers Manage 2018;169:217–27.
[11] Ming T, Yang W, Huang X, Wu Y, Li X, Liu J. Analytical and numerical investigation on a new compact thermoelectric generator. Energy Convers Manage 2017;132:261–71.
[12] Siddique ARM, Kratz F, Mahmud S, Van Heyst B. Energy conversion by nanomaterial-based trapezoidal-shaped leg of thermoelectric generator considering convection heat transfer effect. J Energy Res Technol 2019;141(8):082001.
[13] Zhang QH, Huang XY, Bai SQ, Shi X, Uher C, Chen LD. Thermoelectric devices for power generation: recent progress and future challenges. Adv Eng Mater 2016;18(2):194–213.
[14] Sakamoto T, Taguchi Y, Kutsuwa T, Ichimi K, Kasatani S, Inada M. Investigation of barrier-layer materials for Mg 2 Si/Ni interfaces. J Electron Mater 2016;45(3):1321–7.
[15] Park Y-S, Thompson T, Kim Y, Salvador JR, Sakamoto JS. Protective enamel coating for n-and p-type skutterudite thermoelectric materials. J Mater Sci 2015;50(3):1500–12.
[16] Kraemer D, Sui J, McEnaney K, Zhao H, Jie Q, Ren Z, et al. High thermoelectric conversion efficiency of MgAgSb-based material with hot-pressed contacts. Energy Environ Sci 2015;8(4):1299–308.
[17] Aswal DK, Basu R, Singh A. Key issues in development of thermoelectric power generators: high figure-of-merit materials and their highly conducting interfaces with metallic interconnects. Energy Convers Manage 2016;114:50–67.
[18] LeBlanc S, Yee SK, Scullin ML, Dames C, Goodson KE. Material and manufacturing cost considerations for thermoelectrics. Renew Sustain Energy Rev 2014;32:313–27.
[19] Fabián-Mijangos A, Min G, Alvarez-Quintana J. Enhanced performance thermoelectric module having asymmetrical legs. Energy Convers Manage 2017;148:1372–81.
[20] Xiao H, Gou X, Yang S. Detailed modeling and irreversible transfer process analysis of a multi-element thermoelectric generator system. J Electron Mater 2011;40(5):1195–201.
[21] Reddy B, Barry M, Li J, Chyu MK. Thermoelectric performance of novel composite and integrated devices applied to waste heat recovery. J Heat Transfer 2013;135(3):031706.
[22] Rabari R, Mahmud S, Dutta A, Biglarbegian M. Effect of convection heat transfer on performance of waste heat thermoelectric generator. Heat Transfer Eng 2015;36(17):1458–71.
[23] Aranguren P, Araiz M, Astrain D, Martínez A. Thermoelectric generators for waste heat harvesting: a computational and experimental approach. Energy Convers Manage 2017;148:680–91.
[24] Aranguren P, Astrain D, Rodríguez A, Martínez A. Net thermoelectric power generation improvement through heat transfer optimization. Appl Therm Eng 2017;120:496–505.
[25] Mirhosseini M, Rezaniakolaei A, Rosendahl L. Effect of Heat Loss on Performance of Thin Film Thermoelectric; A Mathematical Model. Materials Research Express. 2019.
[26] Zebarjadi M. Heat management in thermoelectric power generators. Sci Rep 2016;6:20951.
[27] Zhang Q, Liao J, Tang Y, Ming G, Chen M, Qiu P, et al. Realizing thermoelectric conversion efficiency of 12% in Bismuth Telluride/Skutterudite segmented modules through full-parameter optimization and energy-loss minimized integration. Energy Environ Sci 2017.
[28] Lee H, Sharp J, Stokes D, Pearson M, Priya S. Modeling and analysis of the effect of thermal losses on thermoelectric generator performance using effective properties. Appl Energy 2018;211:987–96.
[29] Jing L, Xiang Q, Ze R, Ma M, Wang S, Xie Q, et al. Thermal and electrical analysis of SiGe thermoelectric unicouple filled with thermal insulation materials. Appl Therm Eng 2018;134:266–74.
[30] Snyder GJ, Toberer ES. Complex thermoelectric materials. Nat Mater 2008;7(2):105–14.
[31] Ghosh S, Margatan K, Ahn CH, Bahk J-H. Radiant heat recovery by thermoelectric generators: a theoretical case-study on hot steel casting. Energy Convers Manage 2018;175:327–36.
[32] Chen G. Theoretical efficiency of solar thermoelectric energy generators. J Appl Phys 2011;109(10):104908.
[33] Mahan G. Inhomogeneous thermoelectrics. J Appl Phys 1991;70(8):4551–4.